

Automated and Subject-Specific Coil Selection for Respiratory Self-Navigation in Coronary MRA

Davide Piccini^{1,2}, Bénédicte Maréchal^{1,3}, Simone Coppo², Jérôme Chaptin², Gabriele Bonanno², Gunnar Krueger^{1,3}, Juerg Schwittr⁴, and Matthias Stuber²

¹Advanced Clinical Imaging Technology, Siemens Healthcare IM BM PI, Lausanne, Switzerland, ²Department of Radiology, University Hospital (CHUV) and University of Lausanne (UNIL) / Center for Biomedical Imaging (CIBM), Lausanne, Switzerland, ³CIBM-AIT, École Polytechnique Fédérale de Lausanne, Lausanne, Switzerland, ⁴Division of Cardiology and Cardiac MR Center, University Hospital of Lausanne (CHUV), Lausanne, Switzerland

TARGET AUDIENCE: MR physicists and engineers interested in image reconstruction, motion correction, coronary angiography, or cardiac imaging.

PURPOSE: As demonstrated in several recent publications, respiratory self-navigation (SN) [1] improves the ease-of-use, scanning time and temporal resolution in whole heart coronary MRA when compared to more conventional navigator-based approaches [2]. SN is often implemented in combination with radial imaging (2D or 3D), as such acquisition techniques provide an intrinsic oversampling of the k-space center and can be easily adapted for respiratory tracking. In SN, the respiratory motion information is directly extracted from the image data in k-space and used to correct for respiratory motion during image reconstruction. Many approaches have been proposed for the extraction of a clean respiratory signal, in which the coil elements used for SN are either manually selected or fixed and dependent on the hardware of the body array coils [3]. Although usually very accurate, the manual selection is time consuming and incompatible with an inline reconstruction on the one hand. On the other hand, the use of a pre-defined and not individually dependent fixed set of coil elements may not be optimally suited for all subjects. In this work, we introduce and describe a method for automated subject-specific coil selection for self-navigation, building on an atlas-based image segmentation technique.

METHODS: Whole-heart 3D SN high-resolution datasets were acquired in a total of 18 patients (14 men, mean age 40±17years). All the acquisitions were performed on a 1.5T clinical MRI scanner (MAGNETOM Aera, Siemens AG, Healthcare Sector, Erlangen, Germany). A total of 30 elements of the anterior and posterior phased-array coils were activated for signal reception. Data acquisition was performed segmented and ECG-triggered with a prototype 3D radial trajectory, adapted to self-navigation [3]. A T₂-preparation pulse was added before each segment to the fat-saturated bSSFP imaging sequence. The self-navigated 3D acquisition started ~4 min after injection of a bolus of 0.2 mmol/kg of Gadobutrol (Gadovist, Bayer Schering Pharma, Zurich, Switzerland). Imaging was performed with the following parameters: TR/TE 3.1/1.56 ms, FOV (220mm)³, matrix 192³, voxel size (1.15mm)³, radio frequency (RF) excitation angle 115°, and receiver bandwidth 900 Hz/Pixel. A total of ca. 12000 radial signal readouts were acquired in a number of heartbeats ranging between 377 and 610, depending on the heart rate of the subject. The trigger delay was set using visual inspection of the most quiescent mid-diastolic or late-systolic period on a mid-ventricular short axis cine image series acquired before the injection. Prior to the high resolution acquisition, a 10-second low-resolution (low res) dataset (TR/TE 2.4/1.2 ms, FOV (220mm)³, matrix 96³, voxel size (2.3mm)³, RF angle 60°, and bandwidth 900 Hz/Pixel, 2583 radial lines) was acquired un-triggered and in free-breathing with the very same 3D radial sequence. Such a dataset was used as the patient specific reference volume for image registration and coil selection. In particular, a coarse segmentation of the heart in the reference low resolution volume is achieved by a simple non-rigid registration step. First, a 3D template mask of an adult human heart was pre-defined in a previously acquired whole-heart template and stored. Such template is then deformed and aligned to each patient low res reference volume by estimating a free-form diffeomorphic displacement field using a fast multi-resolution iterative scheme that maximizes the local correlation between the template and the patient's scan [4]. The template mask is therefore also automatically deformed to adapt to the patient's reference volume, thus providing a subject-specific mask (Fig. 1) with no need for user interaction. Such mask is then applied to the coil-uncombined version of the reference volume and used to compute the respective coil weights as follows: $W_i = \sum P x_{i,mask} / (\sum P x_{i,mask} + \sum P x_{i,out})$, where W_i is the weight of the i-th coil element, and $P x_{i,mask}$ and $P x_{i,out}$ are the intensity values for each pixel of the image volume from the i-th coil, inside and outside the mask, respectively. The coil elements are then ranked in a decreasing order, where the highest weights indicate the best visualization of the signal from the heart, and, hence, the best choice for the SN algorithm. The automated selection of the first four ranked coil elements was compared to the manual selections of such first four elements performed by three experienced reviewers using a two-tailed paired student's t-test, adjusted for multiple comparisons. Similarly, the agreement among the reviewers was also tested. Image quality of each coronary segment in datasets obtained with SN correction using the coils from the automated coil selection was compared to that of the datasets reconstructed using a fixed selection which makes use of the four centermost coil elements of the body array coil (Fixed Coils). Such comparison was performed using consensus image quality grading of two experts on a scale from 0 (not visualized) to 4 (sharp borders) [5]. Using this grading and for the automated selection, image quality obtained with the sum of squares of the first four ranked coils (Auto 4 Coils) and the first two (Auto 2 Coils) was also compared.

RESULTS: The average agreement between the three reviewers was 76% on the selection of the four best coils. No statistically significant difference for best coil selection was found among the reviewers. Similarly, the agreement of the algorithm for automated coil selection was on average 71% with all the reviewers (Fig. 2), also with no significant difference. The image quality of almost all coronary segments in the datasets reconstructed with the automated coil selection improved relative to that of the fixed coil selection as shown in Tab. 1. The improvement was statistically significant (*= p<0.05) for the left main segment (LM), the mid right coronary artery (RCA) and left anterior descending artery (LAD). Statistical significance was not reached for the left circumflex (LCX) and the other segments of RCA and LAD.

DISCUSSION AND CONCLUSIONS: The proposed algorithm for the automated ranking of the coil elements enables a fast subject-specific selection of the coils to be used for self-navigation, while motion correction can still be performed inline. Although a 10-second extra scan is needed, no manual user interaction is required. The automated coil selection performs equally well as a manual selection performed by expert reviewers. The results obtained using the proposed algorithm show an improvement in the average image quality of almost all the coronary segments when compared to a fixed selection of the coils. As the coil selection algorithm is based on the percentage of signal from the heart detected by each coil element, the automated ranking of these elements can also be used to decrease the effects of noise or undersampling artifacts by automatically eliminating signal contributions from coils that have the lowest weighting and that are located distant from the prescribed FOV. In particular, for radial imaging, a reduction of the streaking artifacts from bright structures, inside or outside the FOV, may be obtained.

REFERENCES: [1] Stehning C, et al, MRM 2005; 54:476-480; [2] Ehman RL, et al, Radiology 1989; 173:255-263; [3]. Piccini D, et al, MRM 2012; 68:571-579; [4] Chef'd'hôtel C, 2002; In Proc. IEEE ISBI; [5] McConnell MV, et al, AJR 1997; 168:1369-1375.

Coronary Segment	LM:	LAD		
		Prox	Mid	Dist
Fixed Coils	1.9±1.1*	1.7±0.9	1.3±1.2*	0.9±1.0
Auto 4 Coils	2.0±1.1	2.0±1.1	1.4±1.2	1.0±1.2
Auto 2 Coils	2.2±1.1*	1.9±1.2	1.6±1.1*	0.8±1.0

Coronary Segment	Prox LCX	RCA		
		Prox	Mid	Dist
Fixed Coils	1.1±1.3	1.9±1.2	1.5±1.4*	1.0±1.4
Auto 4 Coils	1.2±1.3	2.0±1.3	1.8±1.4*	1.1±1.3
Auto 2 Coils	1.2±1.2	2.1±1.3	1.8±1.4*	1.0±1.3

Table 1: Results of the consensus grading.

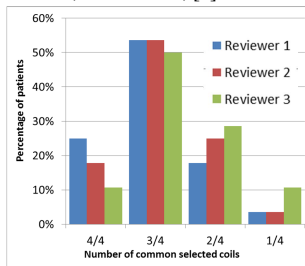


Fig.2: Agreement between the automated algorithm and the three reviewers for all datasets.

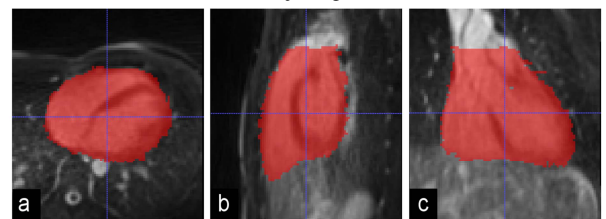


Fig.1: Example of the 10-second low res 3D dataset in axial (a), sagittal (b) and coronal (c) views in one of the patients. The red area overlapping the images is the subject specific 3D mask resulting from the automated segmentation procedure.

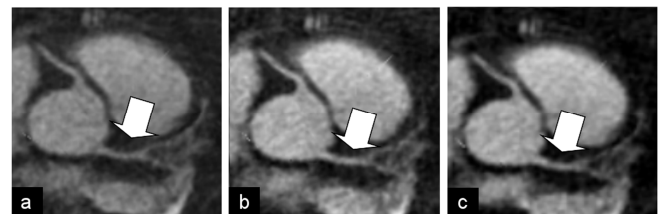


Fig.3: Example of multiplanar reformats of one of the patients using fixed coils (a), the four best automatically ranked coils (b), and the two best (c). A slight improvement of the LM delineation (white arrows) can be observed when comparing (b) and (c) with (a).